International Journal of Coal Science & Technology (2023) 10:38
https://doi.org/10.1007/s40789-023-00599-0

RESEARCH

Novel concepts of mechanical technology for gas recovery from marine hydrate reservoir

Yuting Men[1] · Zhen Song[1,2] · Ying Sun[1] · Kaili Li[1] · Xianlin Qing[1] · Hongen Sun[1] · Meng Zhou[3]

Received: 25 October 2022 / Revised: 6 January 2023 / Accepted: 13 June 2023

Abstract
According to the characteristics of marine natural gas hydrate, China has proposed the solid-state fluidization exploitation technology or natural gas hydrate, with subsea exploitation being key to the commercial recovery of gas. In this paper, two new integrated tools are proposed for breaking and collecting natural gas hydrate, and their working principles and steps are illustrated. Finite element analysis, three-dimensional modeling, and simulations were conducted for both exploitation tools to verify their technological feasibility. The results show that the two exploitation tools can effectively improve the efficiency of hydrate exploitation and ensure the stability of the hydrate reservoir. This provides a reference for further research on the solid-state fluidization exploitation technology of marine gas hydrates.

Keywords Marine natural gas hydrate · Solid-state fluidization exploitation · Exploitation tools · Breaking · Finite element simulation

1 Introduction

Natural gas hydrate, commonly known as flammable ice, is ice-like clean energy produced in high-pressure and low-temperature environments, which is mainly distributed in seabed sediments and terrestrial permafrost (Li and Han 2021; Sakurai et al. 2017). Marine natural gas hydrate resources are distributed globally, and the amount of such resources is more than 100 times that of the terrestrial permafrost. It is regarded as an important energy source in the twenty-first century, and the prospect of resource exploitation is very broad.

According to the existing examples of natural gas hydrate exploitation in various countries, the main exploitation methods of natural gas hydrates include heat stimulation, depressurization, chemical injection, and CO_2 replacement (Yanhong et al. 2021; Chen et al. 2022).

Natural gas is released through hydrate de-composition or replacement (Zhao et al. 2021). In 1969, the Soviet Union successfully exploited the world's first permafrost hydrate reservoir by depressurization and chemical injection methods in the Messoyakha gas field (Collett and Ginsburg 1998, 2000). From 2002 to 2008, Japan, Canada, and other countries carried out three trial exploitation research in the Mallik area by depressurization and heat stimulation methods (Dallimore and Collett 2005; Zuo and Yi 2017; Yamamoto and Dallimore 2008). In 2012, the United States conducted a hydrate exploitation test on the northern slope of Alaska by CO_2 replacement and depressurization methods (Ruprecht et al. 2015). In 2011, P. R. China carried out several hydrate exploitation tests in the Qilian Mountain by a variety of methods (Zhu et al. 2021). In 2013 and 2017, Japan carried out two hydrate exploitation tests in Nankai Trough by depressurization method, which was the first successful exploration of marine natural gas hydrate in the world (Yamamoto et al. 2014). In 2017, P. R. China has carried out a hydrate exploitation test by depressurization in the South China Sea (China Geological Survey 2017; Wu et al. 2017; Ye et al. 2018). From 2019 to 2020, China Geological Survey conducted the second gas hydrate depressurization test extraction in the Shenhu area of the South China Sea

✉ Zhen Song
zhen.song@rwth-aachen.de

1 School of Mechanical Engineering, Southwest Petroleum University, Chengdu 610500, Sichuan, China

2 Sichuan Science and Technology Resource Sharing Service Platform of Oil and Gas Equipment Technology, Chengdu, China

3 School of Sciences, Southwest Petroleum University, Sichuan 610500 Chengdu, China

Published online: 13 July 2023

with a depth of 1225 m (Ye et al. 2020; China Geological Survey 2020).

The heat stimulation and chemical reagent injection method are not suitable as the main exploitation methods of natural gas hydrate due to their limited production efficiency and high cost (Zhang et al. 2008; Li et al. 2015). They are more suitable as an auxiliary exploitation measure. The CO_2 replacement method has the advantages of reducing the risk of geological disasters and storing CO_2 to alleviate the greenhouse effect, but the low replacement rate and replacement efficiency restrict the application of the method (Wei et al. 2022; Zhao et al. 2012; Yanhong et al. 2021). The depressurization method does not need continuous excitation; and is considered to be a potential and economic method for the exploitation of natural gas hydrate (Sun et al. 2019; Wan et al. 2020). However, the problems are the second generation of hydrate, low exploitation efficiency, and geological engineering disasters such as submarine landslides and wellbore instability (Wu et al. 2018). Therefore, in 2012, Zhou Shouwei et al. put forward the solid-state fluidization exploitation method of natural gas hydrate in the shallow surface of deep water (Zhou et al. 2014a, b, 2017; Wei et al. 2018; Qiu et al. 2020), which is using mechanical technology to break the solid hydrate reservoir into fine particles; and then pump the slurry to the offshore platform through the enclosed pipeline for post-processing (Wang et al. 2018a, b). Finally, the separated sediment is supplemented with an appropriate amount of sea sand and backfilled into the goaf area, trying to maintain the original appearance of the seabed as much as possible. In 2017, depending on the "marine Oil 708" deep-water engineering survey ship, China National Offshore Oil Corporation successfully carried out the first global solid-state fluidization exploitation of marine natural gas hydrate at Liwan 3 Station in the north of the South China Sea, using fully independently developed technologies, processes, and equipment. This operation has preliminarily verified the feasibility of the solid fluidization method for the exploitation of marine natural gas hydrate at the technical level (Zhou et al. 2017a, b, 2018). The trial tool of exploitation is a jet nozzle. The jet diameter of the tool is small, only 0.5 m, which is not suitable for hydrate exploitation on a large scale and scope (Wang et al. 2018a, b, 2017).

The integrated equipment for crushing and collecting hydrate is a specific implementation technology based on solid-state fluidization, and the related supporting technology research in various countries is quite a few. To solve the problems of existing exploitation tools and methods, two new exploitation tools which can be applied to the solid-state fluidization exploitation methods are proposed in this paper, which is an umbrella-like tool and a broaching tube that can be used to break and collect hydrate. According to the exploitation conditions, the three-dimensional structural models of the two exploitation tools are established respectively, and the finite element simulation is carried out, which proved the technological feasibility of the two exploitation tools.

2 Umbrella-like tool

2.1 Exploitation process

The exploitation process using the umbrella-like tool includes five steps:

(1) The horizontal well was drilled and the appropriate completion method was selected. After the completion, the umbrella tool was put downward;
(2) When the tool reaches the specified working position, torque and forward thrust are applied to the outer tube rod, while the inner tube rod at the end of the horizontal well remains stationary. Rotate and unfold the umbrella-like tool slowly, make the blade reach the best cutting angle under the control of the elastic positioning lock block;
(3) Pull back the tool to collect hydrate particles while breaking the hydrate reservoir, and transported them to the offshore platform for post-processing such as separation. The separated sediment is flowed back through the internal hose of the tube rod and backfilled to the goaf;
(4) Put downwards the closing tool to close the umbrella-like tool and recover the tool after the exploitation. (Fig. 1)

2.2 Tool design

According to the exploitation principle of the tool and the existing drilling process parameters, the overall structure of the umbrella-like tool is shown in Fig. 2. It is mainly composed of the outer tube rod, inner tube rod, blade, and piston

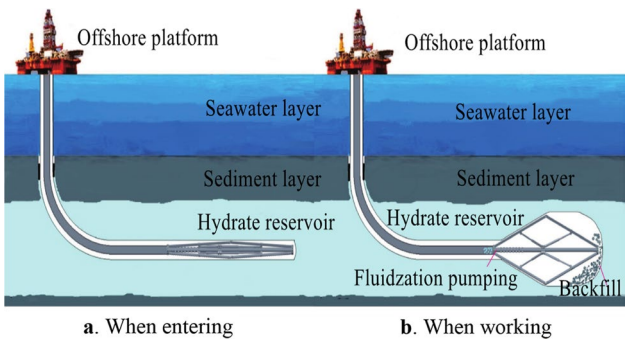

Fig. 1 Working state diagram of umbrella-like tool

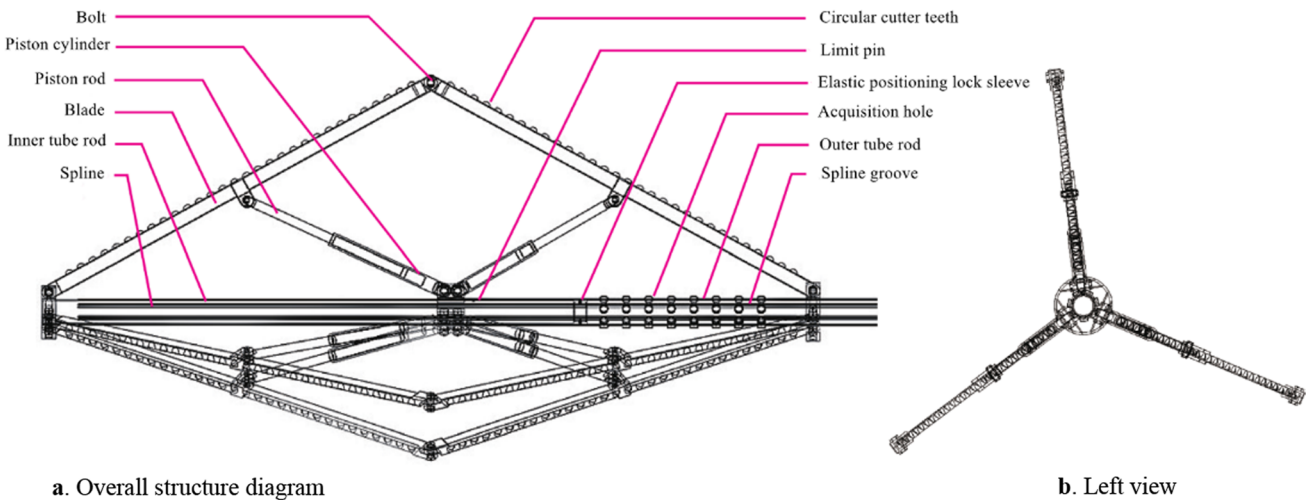

Fig. 2 Structural diagram of umbrella-like tool

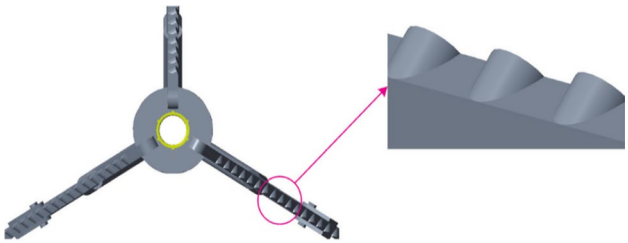

Fig. 3 Schematic diagram of the blade and cutting

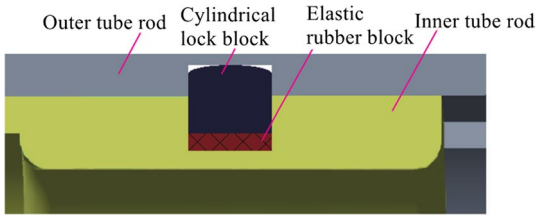

Fig. 4 Structural diagram of the elastic positioning lock sleeve

rod. The inner tube rod is embedded in the outer tube rod and connected by splines, and the two can slide relatively in the axial direction. The outer tube rod is provided with acquisition holes. The blades are connected with the inner tube rod and outer tube rod by hinges, and the piston rods are assembled in piston cylinders.

Considering the resistance of the umbrella-like tool in the exploitation process and the diameter of the outer tube rod, three groups of blades are designed, and the included angle between each group of blades was 120°. To ensure the realization of commercial exploitation efficiency, the length of each blade is designed to be 3.6 m. At the same time, taking into account its function of rotary crushing, the shape of the cutting teeth on the blade is designed as circular teeth, which are at a certain angle with the horizontal plane of the blade, to enhance its shear and extrusion resistance (Fig. 3).

The outer tube rod and the inner tube rod are both hollow, and both are connected in the form of splines to maintain their synchronization during rotation operation, and the backfilling operation can be performed in the tube. Before running the umbrella-like tool, to prevent the outer tube rod and the inner tube rod from sliding relative to each other, several limit pins are used to lock both. When the tool reaches the specified working position, the end of the inner tube rod is in contact with the end face of the horizontal well, and the torque force and thrust are applied to the outer tube rod through the offshore platform. So that the limit pin is cut off under the shearing force. The inner tube rod is blocked and remains stationary in the horizontal direction, while the outer pipe rod continues to move forwards and rotate the blade. When the outer tube rod extends to the optimum cutting angle of the blade, the cylindrical lock block installed in the elastic positioning lock sleeve on the inner tube rod is clamped into the groove of the outer tube rod under the expansion action of the elastic rubber block (Fig. 4), so as to realize the positioning of the exploitation tool after unfolding.

Once the blades are fully deployed, the umbrella-like tool can start the cutting operation. The tool continues to rotate and is pulled back by the connected drill tube. At the same time, the crushed hydrate fine particles are collected by the acquisition hole on the outer tube rod, and transported to the offshore platform through sealed fluidization and other processes. The gas–liquid–solid three-phase separation is carried out on the platform, and the separated sediment passes

Fig. 5 Three-dimensional model of the umbrella-like tool

a. Working state **b**. Non-working state

through the hose and is backfilled with the end of the inner tube rod as the outlet. After the exploitation of the hydrate reservoir is completed, the umbrella-like tool will be closed and drawn back. The working principle of the closing tool is similar to a switchable sliding sleeve device (Yang et al. 2015; Cui et al. 2017). The closing tool is connected through the sucker rod; and lowered into the outer tube rod cavity. Because the outer diameter of the closing tool is larger than the inner diameter of the shoulder at the right end of the inner tube rod. With the operation on the offshore platform, a sufficient forward thrust is applied to the sucker rod, the cylindrical lock block is sheared, and the exploitation tool is retracted and closed.

The three-dimensional model of the umbrella-like tool in the working and non-working status is shown in Fig. 5.

2.3 Overall Steady-state analysis of umbrella-like tool

2.3.1 Physical model establishment

The three-dimensional physical model of the umbrella-like tool is established, and the static analysis of the dynamic transmission part under the condition of bearing torque is carried out using the finite element method (Fig. 6). The physical model is simplified to some extent, but the stress concentration generated in the structure is not neglected. The property parameters of structural steel (Table 1) are directly used in the model to approach the actual situation of umbrella tools. For different parts of the physical model, the density of mesh division is also different. The mesh division of the inner tube rod, outer tube rod, and blade wings is

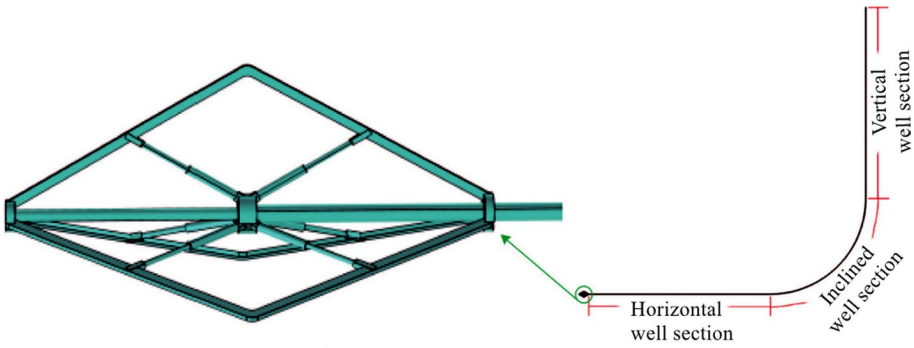

Fig. 6 3D physical model diagram

a. Umbrella-like tool in working state **b**. Power transmission part

Table 1 Parameters of structure steel (Zhang et al. 2005)

Material Brand	Density (kg/m^3)	Young's modulus (GPa)	Poisson's ratio	Yield strength (MPa)	Torsional stiffness (MPa)	Tensile strength (MPa)	Application site
30CrMo	7.90	209	0.28	500	185	710	The hinged part of the piston cylinder and the outer tube rod
45 steel	7.85	200	0.30	355	124	600	Other

relatively sparse, while the mesh division of the connections of each part is denser. In this study, the established physical model is divided into free tetrahedral meshes, and the finite element mesh model is obtained (Fig. 7).

According to the actual working conditions of exploitation tools and hydrate reservoir characteristics (Table 2), the constraint conditions that need to be added during the finite element calculation of the umbrella-like tool in the working state include the load on the blade from the hydrate reservoir (The resultant force of the pressure in the vertical direction and the resistance in the pull-back direction); and the cutting resistance of the cutting teeth during the rotation of the tool. According to the Evans mechanical model (Zhang et al. 2014; Evans 1962), the cutting resistance is estimated to be about 1.6×10^5 N. The blade load is 17 MPa (Zhao et al. 2018). Based on the consideration of the symmetry of the physical model and the control calculation scale, only one group of blades is added with the corresponding boundary load, and the outer boundary of the inner tube rod of the exploitation tool is set as the fixed boundary as the constraint condition.

For the dynamic transmission part, torque calculation is also required based on the above conditions. In the finite element calculation, the torque is added to the connecting drill pipe at the upper end of the drill pipe, and fixed constraints are added to the end face close to the exploitation tool, to analyze whether the whole drill pipe will be twisted during operation.

The umbrella-like tool is connected to the drill string. In the process of exploiting broken hydrate, once its natural frequency is the same or close to the excitation frequency of the vibration, it will cause resonance, resulting in the destruction and failure of the tool structure. Therefore, as an important part of the whole solid-state fluidization exploitation process, in order to avoid resonance during the working process of the tool, make the structural design of the umbrella-like tool more reasonable, and improve the reliability of the umbrella-like tool, it is necessary to conduct modal analysis and research on them. The structural model of the tool adopts the umbrella tool model established in the static analysis. Because the umbrella-like tool is not in a free and unconstrained state when working, it is necessary to add displacement constraints to the model when conducting modal analysis, and the displacement constraints are the same as the boundary conditions of the umbrella tool when working.

2.3.2 Analysis of simulation result

Through the simulation, the equivalent stress distribution of the umbrella-like tool during the operation was obtained, as shown in Fig. 8. The umbrella-like tool has no permanent deformation or fracture in its overall structure in the working condition. The maximum stress of the tool is at the joint between the piston cylinder and the pipe string, about 459 MPa, which does not exceed the yield strength 500 MPa of the steel used in this part. The whole blade is bent, but it does not affect the rotation of the tool to cut hydrate, only affects the actual cutting diameter. In addition, stress concentration also exists in the fixed hinge between the blade and the piston rod. Steady-state analysis of the whole drill

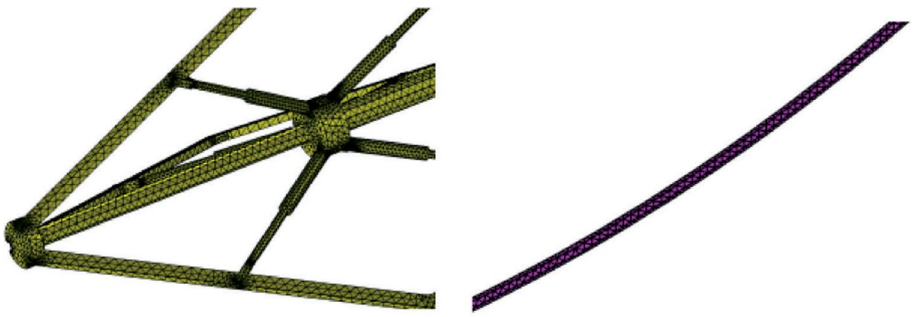

Fig. 7 Finite element meshing diagram

a. Umbrella-like tool local mesh

b. Local mesh of the power transmission part

Table 2 The reference value of hydrate reservoir characteristics (Jun et al. 2019; Liu et al. 2017; Wu et al. 2010)

Depth (m)	Burial depth (m)	reservoir density (kg/m^3)	Elastic Modulus (MPa)	Hydrate porosity (%)	Poisson's ratio	Cohesion (MPa)	Internal friction angle (°)	Shear strength (MPa)	Compressive strength (MPa)
1274	120–190	2000	600	40	0.25	1.5	20	5	22

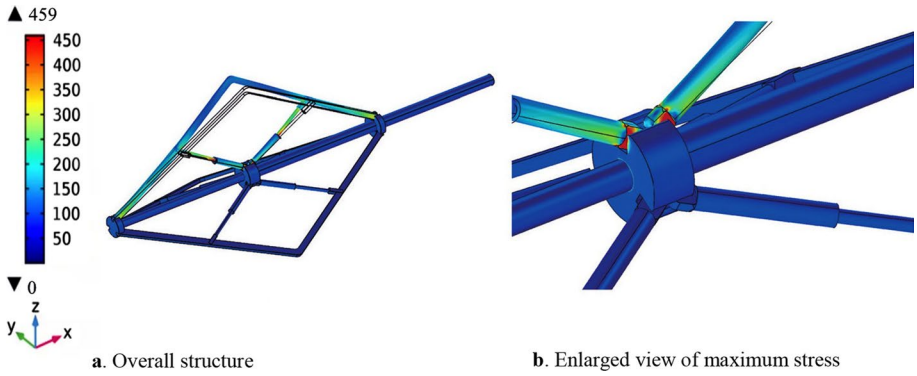

Fig. 8 Equivalent stress distribution diagram

a. Overall structure

b. Enlarged view of maximum stress

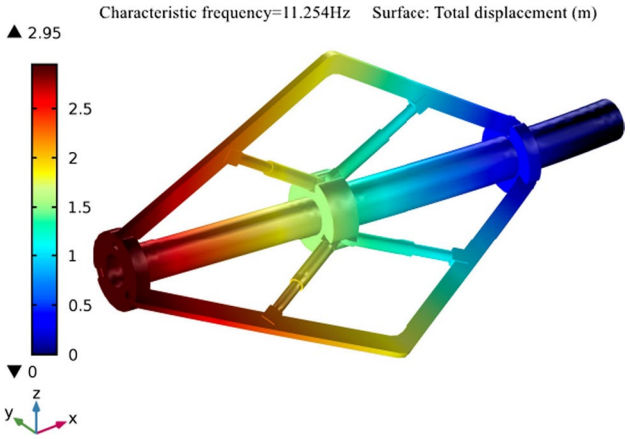

Fig. 9 The first-order mode diagram

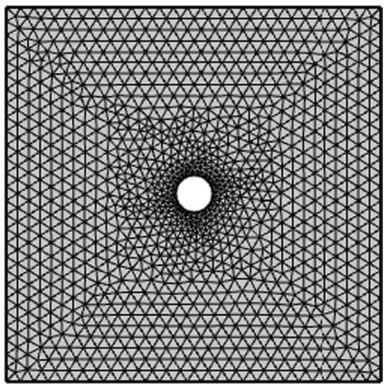

Fig. 10 The grid of the goaf

pipe of the dynamic transmission part during exploitation operation shows that the whole drill pipe has no distortion. The maximum stress of the entire drill pipe is 103 MPa, which is less than the torsional strength of the structural steel (124 MPa) and meets the strength requirements.

According to the vibration theory, compared with the high-order natural frequency, the low-order natural frequency has a greater impact on the configuration of the umbrella-like tool model. In this paper, the first-order natural frequency and vibration mode of the umbrella-like tool is solved. As shown in Fig. 9. The rotational speed of the tool is between 40 and 120 r/min (Zhao et al. 2017, 2018), according to formula 1, the maximum excitation frequency of the umbrella-like tool is 2 Hz, and the minimum natural frequency (11.254 Hz) under working conditions is far greater than the excitation frequency, so it will not cause resonance of the umbrella-like tool model.

$$f = \frac{n}{60} \tag{1}$$

where f is the excitation frequency, Hz; n is the rotation speed of the umbrella-like tool, r/min.

2.3.3 Analysis of stope stability

In order to ensure the economical and efficient exploitation of natural gas hydrate, it is necessary to analyze the stability of the goaf in the gas hydrate reservoir. According to the seabed working conditions, a two-dimensional simulation model of goaf is established. The length of the model is 50 m × 50 m, and the diameter of the goaf is 4 m, as shown in Fig. 10. Assuming that the boundary of the hydrate reservoir is impermeable. Then 15 MPa pressure load (Seafloor pressure and crustal stress) is applied to the upper boundary of the model, the lower boundary is constrained by the displacement in the Y-axis direction, and the left and right boundaries adopt rolling boundaries to balance the force in the horizontal direction of the model (Wang et al. 2012). The reservoir material properties refer to Table 2 of Shenhu Sea Area, northern South China Sea, and the equivalent stress distribution diagram of goaf is obtained through simulation

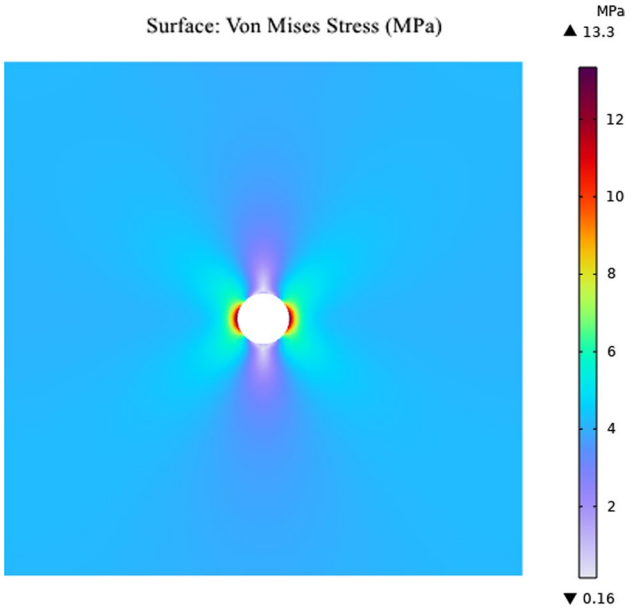

Fig. 11 The equivalent stress distribution

calculation (Fig. 11) The maximum equivalent stress value of 13.3 MPa occurs on both sides of the goaf, which does not exceed the peak compressive strength of the reservoir by 22 MPa (Table 2). Therefore, in the process of exploitation, the goaf of the hydrate reservoir will not collapse.

2.3.4 Technical and economic feasibility

Based on the large-scale physical simulation experiment system of solid-state fluidization exploitation of marine natural gas hydrate, Zhao Jinzhou et al. conducted high-efficiency hydrate crushing experiments (Zhao et al. 2017, 2018), studied the influence laws of different mechanical crushing process parameters (rotational speed between 40 and 120 r/min), cutter head diameter (between 500 and 800 mm), and other factors on hydrate crushing under the condition of 1200 m water depth and established the engineering layout for the mechanical crushing of marine natural gas hydrate samples. Firstly, white solid hydrate deposits are prepared and submerged in the cooling seawater. Then, the hydraulic cylinder lowers the cutter head to the hydrate surface; and then turned on the motor to drive the cutter head to rotate. The hydrate deposits are cut into particles under the action of the cutter head. The experiment verified the technical feasibility of the rotary cutting technology of the umbrella tool. The maintenance cost of the tool is low, similar to the drilling tool, which is a steel structure part. Considering the material, size, and processing method, the cost is not high, if the damage is too serious to repair, the tool can be replaced directly.

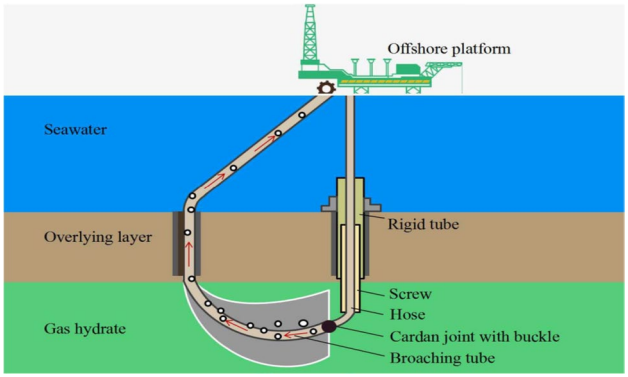

Fig. 12 Schematic diagram of broaching mining

According to an analysis report from China National Offshore Oil Corporation, the economic feasibility standard for the exploitation of marine natural gas hydrate is that the daily output of a single well exceeds 12×10^4 m^3. Take the conservation values of hydrate reservoir parameters (porosity 40%, hydrate saturation 40%), recovery ratio 0.35, and the volume ratio of pure hydrate to gas production is 1:164 (Li et al. 2018). Then the daily output of natural gas can be calculated by the following formula (Wang et al. 2018a, b):

$$V = 1440 \times A \times H \times P \times S \times E \times \eta \tag{2}$$

where V is daily gas production, m^3/d; A is the cross-sectional area of the hydrate reservoir, m^2; H is the exploitation length of the tool, m; P is the porosity of the hydrate reservoir, %; S is the hydrate saturation, %; E is the volume equivalent of gas hydrate decomposed into natural gas per unit; η is the acquisition efficiency of the tool, %.

With the exploitation height of the tool is 4 m, the drawing back speed of the tool is 0.8 m/min (Zhao and Zhang 2005), and the diameter of the wellbore is 0.5 m, the exploitation amount per unit time of the tool can be calculated, that is, the crushing volume rate is:

$$v_0 = \frac{AL}{t} = \frac{\pi(4^2 - 0.5^2)L}{4t} \tag{3}$$

where L is the broken reservoir length of the exploitation tool, m; t is the working time of the exploitation tool, min.

In summary, the daily production of natural gas corresponding to the umbrella-like tool can be estimated: as $V=13.93\times10^4$ m^3/d, which meets the economic requirement of commercial exploitation.

3 Broaching tube

Referring to the long-wall mining technique in coal mining, by reconstructing its main process and key supporting tools, a broaching technology was proposed for increasing the exploitation rate of the hydrate reservoir, and an exploitation tool broaching tube is designed. as shown in Fig. 12.

3.1 Process scheme

First, the hydrate reserve can be divided into multiple stopes, and the process of each stope is similar, mainly including the following 4 steps:

(1) One vertical well is drilled until the interface between the hydrate reservoir and the underlying layer stops;
(2) Two inclined wells with an included angle of 45° are drilled at a certain distance from the vertical wellbore, the endpoint of the inclined wells is positioned on the vertical well at the bottom of the hydrate reservoir;
(3) The special broaching tubes are used to broach the hydrates, while the slurry mixture produced by broaching is collected and transported to the offshore platform to obtain natural gas and the remaining slurry;
(4) Add an appropriate proportion of mud and sand to the remaining slurry after the separation for goaf filling.

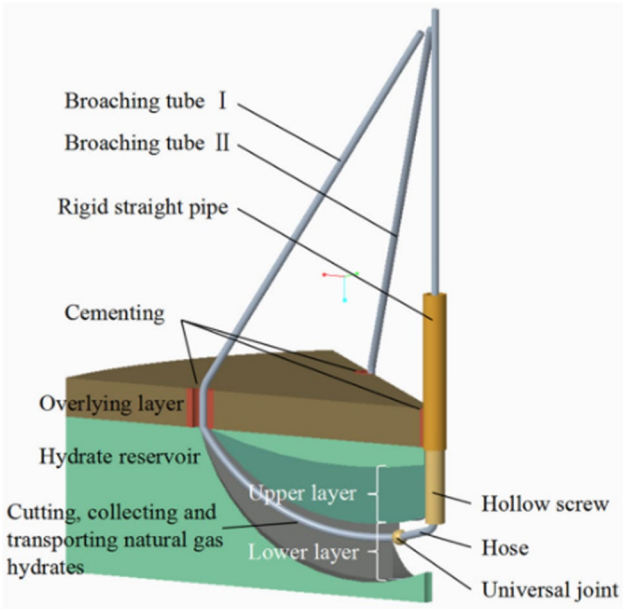

Fig. 13 Reservoir environment

3.2 Working principle

As shown in Fig. 13, the target reservoir is divided into upper and lower layers for layered exploitation. The tool of broaching exploitation is mainly composed of two broaching tubes, a flexible hose, a rigid pipe, and a hollow screw. The rigid pipe is fixed on the seabed and connected with the screw through threads. The two broaching tubes penetrate through the inclined well and are connected with smooth hoses penetrating from the hollow screw through universal joints with buckle. The broaching tubes and hose can be lifted upwards and downwards by the offshore platform.

During broaching, the hydrate reserve is first cut off in the vertical direction along the contact surface between the hydrate and the tube. When a vertical cut finishes, the broaching tubes will be pulled backward and tensioned on the new contact surface; and starts a new cycle of broaching. With the universal joint as the apex; and two broaching tubes as two edges, the hydrate particles can be broached from the hydrate reservoir repeatedly, like "slice by slice", by a reciprocating movement of the universal join in the vertical direction.

Figure 14 is a drawing of the broached tube designed concerning the structural characteristics of the broach (Pu et al. 2016). During the broaching process, the cutter teeth cut the hydrate reservoir to obtain a mixture that is sucked into the pipe by the collection hole on the broached tube body under negative pressure. If the negative pressure in the tube is adjusted to an appropriate range, the hydrate particles can be completely decomposed in the tubes and uplifted to the offshore platform through the sealed pipe. When the resistance of mud and sand is too high in the process of exploitation, the pumping pressure in the broaching tube can increase to decompose the hydrate around the collection hole outside of the broaching tube. This can lead to the hydrate reservoir being relatively softer and less dense, thus reducing the force resistance and facilitating the broaching process.

The details of the broaching process are illuminated as below:

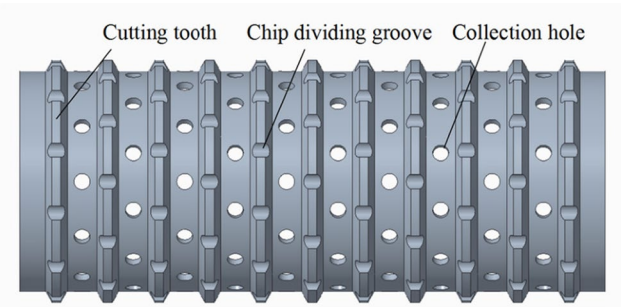

Fig. 14 Special broaching tube

(1) Two broaching tubes pass through the inclined well, while the hose passes through the hollow screw, and the broaching tube head is clamped into the double-cross universal joint with a buckle on the smooth hose head. The connection of the broaching tool is completed;
(2) The lower layer exploitation is carried out. The offshore platform applies the same pulling force to the two broaching tubes; slowly lowers the hollow screw and hose while lifting the broaching tube; so that the two broaching tubes and the hydrate reservoir slide relative to each other. This is forward exploitation, as shown in Fig. 13. In the process, the internal pressure inside of the broaching tube keeps negative, to collect the slurry mixture. Then slowly lower the broaching tube, so that the hollow screw and hose go up, and complete the reverse exploitation. In this way, until the upper design limit position of the lower layer is reached, a broaching process is completed;
(3) After the lower layer is mined to the designed size, the goaf of the lower layer is immediately filled with pressure grouting from the inclined well, and the hydrate reservoir of the upper layer is exploited at the same time;
(4) When the upper layer exploitation is completed, the tools are recovered, and the upper layer goaf is filled in time. Figure 15 shows the V-shaped vertical goaf finally formed by layer exploitation;
(5) While filling the upper layer, all of the above steps can be repeated in the opposite direction of the stope. Until the hydrate reservoir around the vertical well forms the "blossom shape" stope area as shown in Fig. 16. The number in the figure represents the broaching sequence.

3.3 Feasibility analysis

3.3.1 Mechanical behavior analysis of broaching tube

The designed broaching tube should be ensured to safely pass through the inclined well and work without failure. Based on the actual average thickness of 60 m, which is the average thickness of the reservoir in the Shenhu area of the South China Sea. The trajectory of the inclined well is approximated as a one-sixth arc with a radius of 100 m. The broaching tube has an outer diameter of 0.3 m and a wall thickness of 10 mm. The stress analysis is only performed

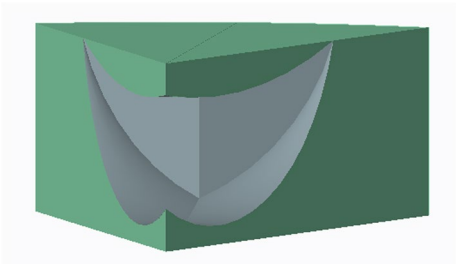

Fig. 15 Goaf illustration

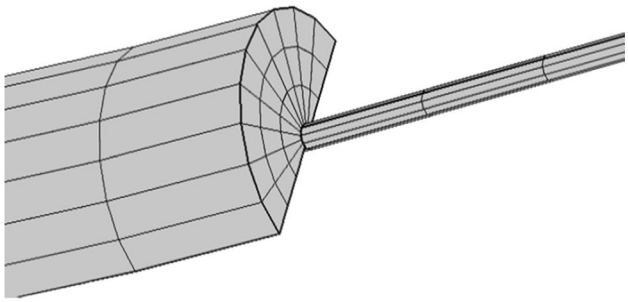

Fig. 17 The grid details

Fig. 16 Ideal shallow goaf mode

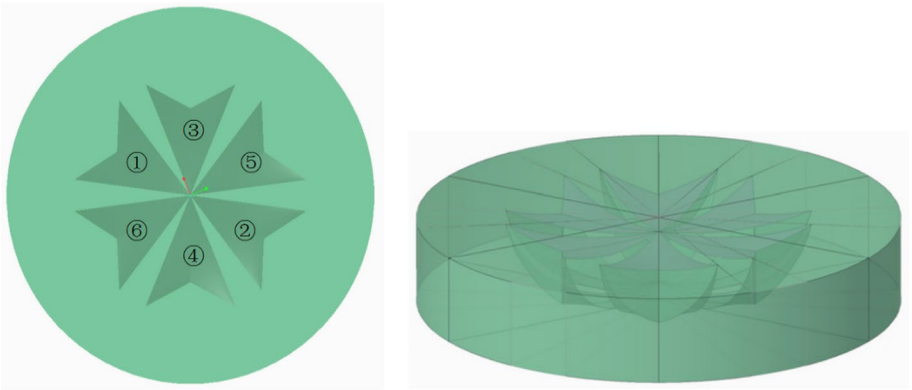

a. Exploitation sequence **b**. The overall appearance of the stope area

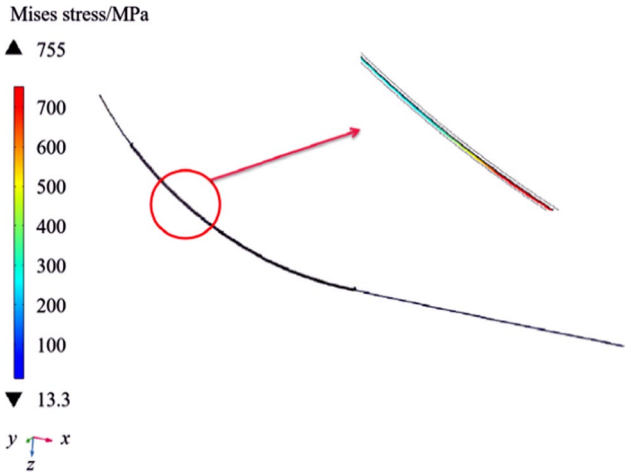

Fig. 18 Stress cloud map of the tubing during exploitation

on the contact face of the inclined well and the broaching tube (Fig. 17).

The stress state of the broaching tube is analyzed by using the basic theory of multi-body dynamics. The broaching tube is defined as a linear elastic mechanic model. The front ends of the broaching tube are given a specified displacement constraint in the inclined well along with the axis trajectory, and pass through the inclined well for a certain distance. The broaching resistance (Zhang et al. 2014; Evans 1962) along the tube is estimated to be 210 kN, and the vertical load from the above hydrate reserve to the broaching tube is 16 MPa. The broaching process requires the material of the broaching tube to have sufficient toughness, plasticity, and wear resistance, so 40Cr is selected as the material of the broaching tubes. The related properties of the material include elastic modulus 211 GPa, Poisson's ratio 0.277, density 7.85×10^3 kg/m^3, and yield limit 785 MPa.

Von-Mises stress is used to determine whether the broaching tube enters the plastic state (Zhang 2016). As shown in Fig. 18, there is obvious stress concentration in the middle of the broaching tube entering the inclined well section. The equivalent stress is smaller as it moves farther away from the middle position. The process of broaching the tube entering the hydrate reservoir is a bending process, its radius of curvature will change from infinity to equal to the inclined well. The maximum equivalent stress value is 755 MPa, which is less than the yield strength of the broaching tube 40Cr, i.e. 785 MPa. It shows that the broaching tube is always inelastic deformation during the process, and will not cause permanent deformation.

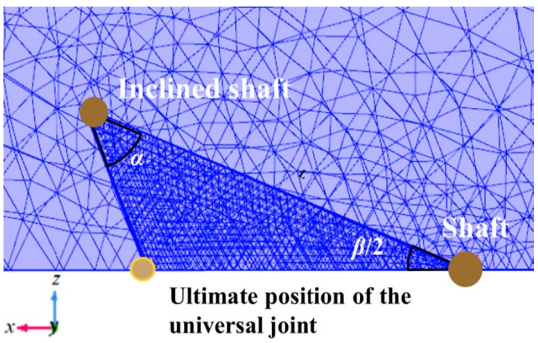

Fig. 19 Top view of goaf

3.3.2 Analysis of stope stability

In order to ensure the economical and effective exploitation of marine natural gas hydrates and reduce safety risks, it is necessary to study the mechanical behavior of stopes with the finite element method. The height of the reservoir model is 60 m. Because the model is symmetric, only half of the domain is modeled to reduce computational costs. The following Fig. 19 shows the top view of the model.

The distance between the inclined well and the vertical well and the limit position of the universal joint determine the shape and volume of the goaf. $\angle\alpha$ is the broaching angle, L is the broaching radius, and $\angle\beta = 45°$ is the angle between the two inclined wells. In order to reduce the computational cost of the model, a structured grid is selected, and the grid around the stope is refined to ensure the accuracy of the grid.

The stress distribution and the seafloor settlement are important parameters to judge whether the goaf will collapse, and also the primary criteria to determine the size of the stope. Hydrate sediments in the Shenhu area of the South China Sea are mainly argillaceous fine silt (Lui et al. 2012), with small particle size distribution and low intensity. Therefore, the relative parameters of low-strength bentonite used in the study of mechanical properties of hydrate sediments by Li Lingdong et al. (Li et al. 2012) are selected as the finite element calculation parameters (Table 3). The overburden failure is evaluated by the Drucker-Prager criterion and Mohr–Coulomb criterion.

Without considering the supporting effect of the overlying layer, the top of the model bears about 12.86 MPa of seabed

Table 3 Geotechnical mechanical parameters of hydrate (Li et al. 2012)

Parameter	Value
Elasticity modulus (MPa)	749
Poisson ratio	0.32
Density (kg/m^3)	2600
Cohesion (MPa)	1.2
Internal friction angle, $\varphi^{(o)}$	7.2
Biot-willis coefficient	1
Confining pressure (MPa)	16.37

Table 4 Optimization scheme and results of stope shape

Exploitation angle(°)	Maximum shear stress at following exploitation radius (MPa)		
	50 m	55 m	60 m
30	2.43	2.59	2.79
35	2.55	2.85	3.09
40	2.75	3.10	3.14
45	3.15	3.20	3.33
50	3.18	3.25	3.54
55	3.26	3.51	3.60
60	3.70	3.92	4.33

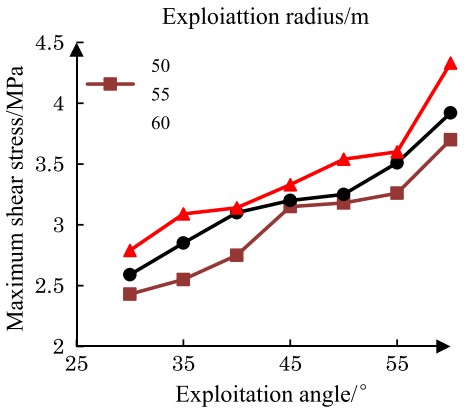

Fig. 20 Maximum shear stress of each stope

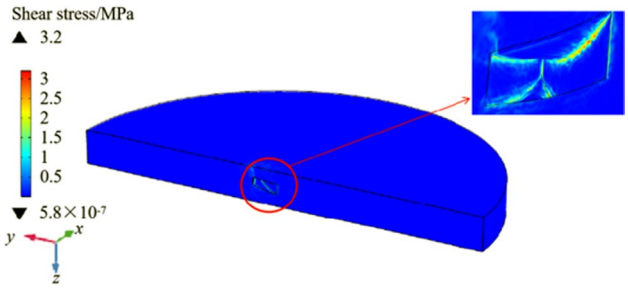

Fig. 21 Shear stress cloud of ideal goaf

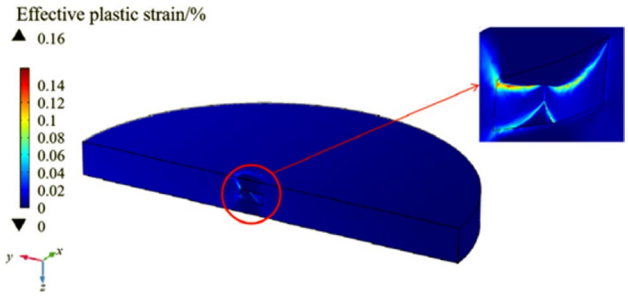

Fig. 22 Ideal goaf effective plastic strain cloud

pressure and 3.51 MPa of formation stress. The reservoir is supported by the foundation, so the displacement constraint in the *y*-axis direction is used at the bottom boundary of the model. Saint Venant's principle holds that the influence of the near-stress concentration on the far distance can be ignored. Therefore, when the research scope of the hydrate reservoir is large enough, the local stress concentration after exploitation will not affect the stress distribution on the side of the model. Therefore, the rolling boundary is adopted on the side of the model to balance the stress of the model in the horizontal direction, and slight deformation is allowed in the vertical direction. The vertical plane of the model uses symmetrical boundary conditions, and the static pressure of the liquid column of 13 MPa is applied on all surfaces inside the goaf.

Table 4 shows the optimization scheme and results of the shape parameters of the stope. The broaching radius is 50, 55, and 60 m respectively, and the broaching angle varies from 30° to 60°, the adjustment range is 5°. Since the damage of overburden is usually a shear failure (Li 2013), the simulation results mainly reflect the shear stress. As shown in Fig. 20 with the increase of the radius and angle, the volume of the stope increases, and the corresponding maximum shear stress increases gradually. According to the Mohr circle and strength envelope of the bentonite sediment sample in reference (Lui et al. 2012), the ultimate shear strength of the sample is 3.27 MPa when the confining pressure is 16.37 MPa. In all stopes where the maximum shear stress is less than the shear strength of the hydrate reservoir, the sizes that correspond to the largest volume are the ideal stope sizes. From the perspective of safety, the ideal goaf shape is finally determined with the exploitation angle of 45° and the exploitation radius is 55 m. Therefore, the volume 12,354 m^3 is finally set as the ideal stope size.

As shown in Fig. 21, there are two stress concentration areas, which are at the start and end positions of the upper arc. The maximum shear stress is 3.20 MPa, which is less than the ultimate shear strength of the hydrate reservoir 3.27 MPa. Therefore, the overlying layer keeps stable and will not collapse. As shown in Fig. 22, there is only slight local plastic deformation with a maximum plastic

deformation of 0.16%. The deformation areas are mainly located at the sharp corner of the goaf.

3.4 Technical and economic feasibility

Broaching exploitation technology is a special technology for hydrate reservoir exploitation, which is proposed with reference to the principle of reciprocating coal cutting by coal planer. Because the geological conditions of coal mines are different from marine hydrate reservoirs, this paper designed a broaching tube for hydrate reservoir exploitation; and verified the scientific nature of this technology through the physical experiment of hydrate efficient breaking. The maintenance cost of the tool is low, similar to drilling tool, it is a steel structure part. Considering the material, size and processing method, the cost is not high, if the damage is too serious to repair, the tool can be replaced directly.

For the broaching process, the main factors affecting the daily production volume are the broaching speed and the speed of reciprocating upwards and downwards. Referring to the drilling speed (Wu et al. 2016) and the rotary rate of the drilling tool (Yan 2001), the broaching speed is 0.8 m/min, and the reciprocating speed is 36 m/min. It takes 126 h to exploit a complete "blossom shape", thus the production rate is 3.27 m^3/min. According to Eq. (2), the daily gas production of broaching is 142,000 m^3. It proves that broaching technology has the potential to be used to exploit the hydrate reservoir.

4 Conclusions

The safe, reliable, and economical exploitation technology of natural gas hydrate is the key to the development and utilization of natural gas hydrate. In this paper, two exploitation tools are designed for the mechanical cutting of solid-state fluidization exploitation. On this basis, the modeling and finite element analysis of the two exploitation tools are carried out, and the technical and economic feasibility of the two exploitation tools are verified. The designed tools have the following four features:

(1) The hydrate breaking and collection can be carried out in a controllable manner while bearing the pressure of the overburden;
(2) The operation process is continuous and stable;
(3) The separated tailings can be backfilled to avoid the collapse of the goaf;
(4) The exploitation can be further optimized to improve the exploitation efficiency.

The research of this paper aims to provide new research ideas and some theoretical basis for the mechanical exploitation of marine natural gas hydrate. In addition to the previous lab-scale experiments, more physical experiments and hydrate trial exploitation will be carried out in the follow-up national key R&D project.

Acknowledgements This work was partially funded by the Postdoctoral Research Foundation of China (2017M623061), the Natural Science Foundation of Hunan province (2020JJ4724), and the Natural Engineering Research Center for Oil & Gas Drilling Equipment (2021-2.3)

Author contributions Zhen Song, and Yuting Men, conceived the idea of the study, Yuting Men, Kaili Li, and Xianlin Qing constructed the model for simulation analysis, Hongen Sun, and Meng Zhou wrote the initial draft of the paper, all authors discussed the results and revised the manuscript.

Funding This work was supported by the China Postdoctoral Science Foundation (2017M623061), the Natural Science Foundation of Hunan province (2020JJ4724), and the Natural Engineering Research Center for Oil & Gas Drilling Equipment (2021-2.3).

Availability of data and materials All the data are presented in the manuscript.

Declarations

Competing interests The authors declare that they have no known competing financial interests or personal relationships that could have appeared to influence the work reported in this paper.

References

Chen XJ, Lu HL, Gu LJ, Shang SL et al (2022) Preliminary evaluation of the economic potential of the technologies for gas hydrate exploitation. Energy 243:0360–5442

China Geological Survey (2020) The second round of trial production of natural gas hydrate in China's sea area succeeded

China Geological Survey (2017) The first test of gas hydrate in sea was completed successfully

Collett TS, Ginsburg GD (1998) Gas hydrates in the messoyakha gas field of the west Siberian basin a re-examination of the geologic evidence. Int J Offshore Polar Eng 8(1):22–29

Collett TS, Ladd J (2000) Detection of gas hydrate with downhole logs and assessment of gas hydrate concentrations (saturations) and

gas volumes on the blake ridge with electrical resistivity log data. Proc ODP Sci Results 164:179–191
Cui ZQ, Qi HF, Ge SQ (2017) A reclosable sleeve device: China. CN205876269U
Dallimore SR, Collett TS (2005) Scientific Results from the Mallik 2002 Gas Hydrate Production Research Well Program, Mackenzie Delta, Northwest Territories, Canada. Bull Geol Surv Canada 585(36)
Evans I (1962) A theory of the basic mechanics of coal ploughing. In: Proceedings of a symposium held at the University of Missouri, pp 761–798
Jun Y, Masato K, Yoshihiro K et al (2019) In situ mechanical properties of shallow gas hydrate deposits in the deep seabed. Geophys Res Lett 46(24):14459–14468
Li YS (2013) Geotechnical mechanics. Wuhan University Press, Wuhan
Li ZF, Han J (2021) Environmental safety and low velocity of the development of submarine natural gas hydrate with examples of test production in South China Sea. Environ Sci Pollut Res 28(5):6259–6265
Li LD, Cheng YF, Sun XJ, Cui Q (2012) Experimental sample preparation and mechanical properties study of hydrate bearing sediments. J China Univ Petrol 36(4):97–101
Li SX, Li J, Cao W (2015) Experimental studies on the effects of hot brine salinity on gas hydrate production. J Chem Eng Chin Univ 29(2):482–496
Li JF, Ye JL, Qin XW et al (2018) The first offshore natural gas hydrate production test in South China Sea, China. Geology 1(1):5–16
Liu CL, Ye YG et al (2012) The characteristics of gas hydrates recovered from Shenhu Area in the South China Sea. Mar Geol 307:22–27
Liu J, Zhang JZ, Sun YB et al (2017) Gas hydrate reservoir parameter evaluation using logging data in the Shenhu area, South China. Sea Natural Gas Geosci 28(1):164–172
Pu YM, Li XH, Yan B (2016) Selection and sharpening of metal cutting tools. Chemical Industry Press, Beijing
Qiu SZ, Wang GR, Zhou SW et al (2020) The downhole hydro cyclone separator for purifying natural gas hydrate: structure design, optimization, and performance. Sep Sci Technol 55(3):564–574
Ruprecht Yonkofski CM, Horner J, White MD (2015) Experimental and numerical investigation of guest molecule exchange kinetics based on the 2012 ignik sikumi gas hydrate field trial. J Natural Gas Sci Eng 35:1480–1489
Sakurai S, Nishioka I, Matsuzawa M et al (2017) Issues and challenges with controlling large drawdown in the first offshore methane-hydrate production test. SPE Prod Oper 32(4):500–516
Sun X, Luo TT, Wang L et al (2019) Numerical simulation of gas recovery from a low-permeability hydrate reservoir by depressurization. Appl Energy 250:7–18
Wan QC, Si H, Li B, Yin ZY et al (2020) Energy recovery enhancement from gas hydrate based on the optimization of thermal stimulation modes and depressurization. Appl Energy 278:115612
Wang TX, Feng ZY (2012) Foundation of soil mechanics, 2nd edn. China Electric Power Press, Beijing
Wang GR, Zhong L, Zhou SW et al (2017) Jet breaking tools for natural gas hydrate exploitation and their support technologies. Nat Gas Ind 37(12):68–74
Wang GR, Huang R, Zhong L et al (2018a) An optimal design of crushing parameters of marine gas hydrate reservoirs in solid fluidization exploitation. Nat Gas Ind 38(10):84–89
Wang B, Dong H, Liu Y et al (2018b) Evaluation of thermal stimulation on gas production from depressurized methane hydrate deposits. Appl Energy 277:710–718
Wei N, Sun WT, Meng YF et al (2018) Multiphase non-equilibrium pipe flow behaviors in the solid fluidization exploitation of marine NGH reservoir. Energy Sci Eng 6(6):760–782
Wei WN, Li B, Gan Q et al (2022) Research progress of natural gas hydrate exploitation with CO_2 replacement: a review. Fuel 312:00016–02361
Wu NY, Yang SX, Zhang HQ et al (2010) Gas hydrate system of Shenhu area, Northern South China sea: wire-line logging, geochemical results and preliminary resources estimates. Offshore Technology Conference, 3–6 May, Houston, Texas, USA.
Wu PC, Xu ZX, Meng YF et al (2016) Transient fluctuation law of bottom hole pressure in formation drilling with narrow safety density window. Drill Prod Technol 39(4):22–26
Wu NY, Huang L, Hu GW et al (2017) Geological controlling factors and scientific challenges for offshore gas hydrate exploitation. Mar Geol Q Geol 5(37):1–11
Wu Q, Lu JS, Li DL et al (2018) Experimental study of mechanical properties of hydrate-bearing sediments during depressurization exploitation. Rock Soil Mech 39(12):4508–4516
Yamamoto K, Dallimore S (2008) Aurora-jogmec-nrcan mallik 2006–2008 gas hydrate research project progress. Fire Ice
Yamamoto K, Terao Y, Fujii T, Terumichi I, et al (2014) Operational overview of the first offshore production test of methane hydrates in the Eastern Nankai Trough. Offshore Technology Conference
Yan TN (2001) Rock and soil drilling engineering. China University of Geosciences Press, Wuhan
Yang DK, Zhu YJ, Tang ZY, Zhang R, Xue ZF (2015) Development and application of reclosable staged fracturing sleeve. China Petrol Mach 43(6):88–91
Yanhong W, Xuemei L, Shuanshi F et al (2021) Review on enhanced technology of natural gas hydrate recovery by carbon dioxide replacement. Energy Fuels 35(5):3659–3674
Yanlong L, Lele L, Yurong J et al (2021) Characterization and development of marine natural gas hydrate reservoirs in clayey-silt sediments: a review and discussion. Adv Geo-Energy Res 5(1):75–86
Ye JL, Qin XW, Qiu HJ, Liang QY et al (2018) Preliminary results of environmental monitoring of the natural gas hydrate production test in the South China Sea, China. Geology 1(2):202–209
Ye JL, Qin XW, Xie WW et al (2020) Main progress of the second gas hydrate trial production in the South China Sea. Geol China 47(03):557–568
Zhang SY (2005) The latest metal material grades, properties, uses and Chinese and foreign brands are quickly used in a practical manual. China Science and Technology Culture Press, Beijing
Zhang SH (2016) Principles of plastic forming mechanics. Metallurgical Industry Press, Beijing
Zhang WD, Liu YJ, Ren SR et al (2008) Thermal analysis on heat injection to natural gas hydrate (NGH) recovery. Nat Gas Ind 5:77–79
Zhang MQ, Jia SS, Zhang JG (2014) Comparison and analysis of predictor methods for rock breaking resistance of bit. Colliery Mech Electr Technol 4:24–28
Zhao JZ, Zhang GL (2005) Drilling engineering technical manual. China Petrochemical Press, Bing
Zhao JF, Xu K, Song YC, et al (2012) A Review on Research on Replacement of CH4 in Natural Gas Hydrates by Use of CO_2 Energies 5(2):399.
Zhao JZ, Zhou SW, Zhang LG et al (2017) The first global physical simulation experimental systems for the exploitation of marine natural gas hydrates through solid fluidization. Nat Gas Ind 37(09):15–22
Zhao JZ, Li HT, Zhang LH, Sun W, Wang G (2018) Large-scale physical simulation experiment of solid fluidization exploitation of marine gas hydrate. Nat Gas Ind 38(10):76–83
Zhao JF, Xu L, Guo XW et al (2021) Enhancing the gas production efficiency of depressurization-induced methane hydrate exploitation via fracturing. Fuel 288:119740

Zhou SW, Chen W, Li QP et al (2014a) The green solid fluidization development principle of natural gas hydrate stored in shallow layers of deep water. China Offshore Oil Gas 26(05):1–7

Zhou SW, Chen W, Li HP (2014b) Solid state fluidization green mining technology for deep water and shallow gas hydrate. China Offshore Oil Gas 26(5):1–7

Zhou SW, Zhao JZ, Li QP et al (2017a) Optimal design of the engineering parameters for the first global trial production of marine natural gas hydrates through solid fluidization. Nat Gas Ind 37(9):1–14

Zhou SW, Chen W, Li QP, Zhou JL, Shi HS (2017b) Research on the solid fluidization well testing and production for shallow non-diagenetic natural gas hydrate in deep water area. China Offshore Oil and Gas 29(4):1–8

Zhou SW, Li QP, Chen W et al (2018) The World's first successful implementation of solid fluidization well testing and production for non-diagenetic natural gas hydrate buried in shallow layer in deep water. Proc Annu Offshore Technol Conf 4:2784–2794

Zhu YH, Pang SJ, Wang PK, Zhang S, Xiao R (2021) A review of the resource potentials and test productions of natural gas hydrates in China. Sediment Geol Tethyan Geol 41(4):524–535

Zuo RQ, Yi LI (2017) The review of mallik ngh successful production tests in Canada's permafrost zone. Explor Eng (rock Soil Drill Tunnel) 44(08):1–12